Available online at www.sciencedirect.com

ScienceDirect

Journal of the European Ceramic Society 28 (2008) 2471–2478

www.elsevier.com/locate/jeurceramsoc

# Effect of thermal treatment on damage mechanical behaviour of refractory castables: Comparison between bauxite and andalusite aggregates

M. Ghassemi Kakroudi[a,b], E. Yeugo-Fogaing[c], C. Gault[b], M. Huger[b,*], T. Chotard[b,*]

[a] *Department of Ceramic Engineering, University of Tabriz, Tabriz 51666-16741, Islamic Republic of Iran*
[b] *Groupe d'Etude des Matériaux Hétérogènes (GEMH), ENSCI, Limoges, France*
[c] *Matériaux à Finalités Spécifiques, EA 3834, Institut des Sciences de l'Ingénieur de Toulon et du Var, Av. G. Pompidou, BP 56, 83162 La Valette du Var Cedex, France*

Received 15 January 2008; received in revised form 20 March 2008; accepted 28 March 2008
Available online 6 June 2008

## Abstract

During service life, refractory castables are subjected to different solicitations. The knowledge of their damage behaviour under such solicitations is highly needed for a better understanding of mechanisms, which induce the final rupture of structures made with refractories. Since these materials are often used as walls of metallurgical tools, thermal gradients in such structure can lead to severe mechanical stresses in the outer layer of the refractory part which is at a rather low temperature.

This study deals with the mechanical properties at room temperature (by tensile test) of two refractory castables treated at different temperatures (110 °C, 250 °C, 500 °C, 700 °C, 900 °C and 1100 °C) in order to reproduce the thermal gradient in walls of metallurgical tools. Two refractory castables are considered: an ultra-low cement content bauxite-based material (Bau-ULCC) and a low cement content andalusite-based material (And-LCC).

*Keywords:* Tensile test; Mechanical properties; Thermal expansion; Refractories; Castables

## 1. Introduction

The use of monolithic refractories in various industries (metallurgical, cement, etc.) is continuously increasing for the last 20 years [1,2]. During their service life, refractory castables are subjected to severe solicitations, especially from a thermomechanical point of view and are degraded by a combination of several mechanisms, mainly thermal shock, abrasion, corrosion and mechanical impact. The behaviour of these materials face to those mechanisms is influenced by the evolution of many factors such as their chemical composition, their microstructure as well as their phase transformation, which occur at high temperature during firing process, and/or in service [3,4].

The physical properties of a refractory concrete are highly temperature-dependent. This is primarily caused by the complex hydration and dehydration reactions of calcium aluminate cement [5–7].

The elaboration of monolithics containing calcium aluminate cements contains several steps such as mixing, placing and consolidation, curing and dry out and finally use in service. Each of these steps within the castable placing chain are intimately linked to the initial hydration process of the calcium aluminate cement (CAC) [8,9].

The refractory castables generally present complex heterogeneous microstructures which can provide strong internal stresses by thermal source. Because of the mismatch between the properties of phases and mainly between their coefficients of thermal expansion, the service conditions can considerably affect their initial microstructural state and thus their thermomechanical properties [10,11].

Previous studies have already been performed in the field of the high temperature behaviour of refractory castables [3,12].

---

* Corresponding author at: Tel.: +33 5 55 45 22 36; fax: +33 5 55 79 09 98.
*E-mail addresses:* marc.huger@unilim.fr (M. Huger), thierry.chotard@unilim.fr (T. Chotard).

0955-2219/$ – see front matter © 2008 Elsevier Ltd. All rights reserved.
doi:10.1016/j.jeurceramsoc.2008.03.048

This paper deals with results of an experimental approach developed to characterise the microstructural changes and damage processes, which occur in such materials during the first heating.

## 2. Materials and experimental procedures

### 2.1. Material and sample preparation

Two commercial castables are considered. The first one is a low cement andalusite castable (And-LCC) made of andalusite aggregates, fumed silica, alumina and of a calcium aluminate cement. The second is an ultra-low cement bauxite castable (Bau-ULCC) made of bauxite aggregates, fumed silica, alumina and of the same cement. Both materials are characterised by the same fumed silica content. In Bau-ULCC, the alumina content is two times higher than in And-LCC. Table 1 shows the chemical compositions of the castables supplied by the manufacturer. The high difference between the silica contents of the two materials is mainly due to the high silica content in andalusite aggregates compared to bauxite ones. For both castables, the maximum aggregate size is about 5 mm. The materials were cured during 24 h at 110 °C. Fig. 1 shows pictures of polished sections of cured materials. After machining, some samples have been fired at 250 °C, 500 °C, 700 °C, 900 °C and 1100 °C in order to simulate several thermal histories before characterisation. These temperature levels have been fixed according to the temperature range representing the refractory castables in specific industrial applications. Firing thermal cycles are characterised by 5 °C/min heating and cooling rates and by a 5 h isothermal dwell at the maximum firing temperature.

### 2.2. Dilatometry

In order to study thermal expansion mismatch effects, samples of matrix and of aggregates have been prepared. The samples of the matrix were prepared by casting and the samples of aggregates (grain size less than 200 μm), were shaped by pressing. The thermal cycles (heating/cooling) were carried out with a slope of 5 °C/min.

The influence of the temperature on a material causes, in general, variations of its apparent volume. The knowledge of these variations makes it possible to characterise many physical phenomena which occur within a material during a given heat treatment. Dilatometric tests were carried out by a dilatometer ADAMEL DI. The samples usually used are of dimension 10 mm × 5 mm × 5 mm.

Table 1
Chemical analysis and characterisations data of the two refractories

| Castable type | And-LCC | Bau-ULCC |
|---|---|---|
| Aggregate type | Andalusite | Bauxite |
| $Al_2O_3$ (wt.%) | 58 | 85 |
| $SiO_2$ (wt.%) | 37.5 | 10 |
| CaO (wt.%) | 2.3 | 1.1 |
| $Fe_2O_3$ (wt.%) | 0.9 | 1 |
| Maximum aggregate size (mm) | 5 | 5 |
| Water requirement (wt.%) | 4.5–5.5 | 4.2–5.2 |
| Open porosity (vol.%) | 6 | 10 |
| Apparent density (kg/m$^3$) | 2600 | 2970 |

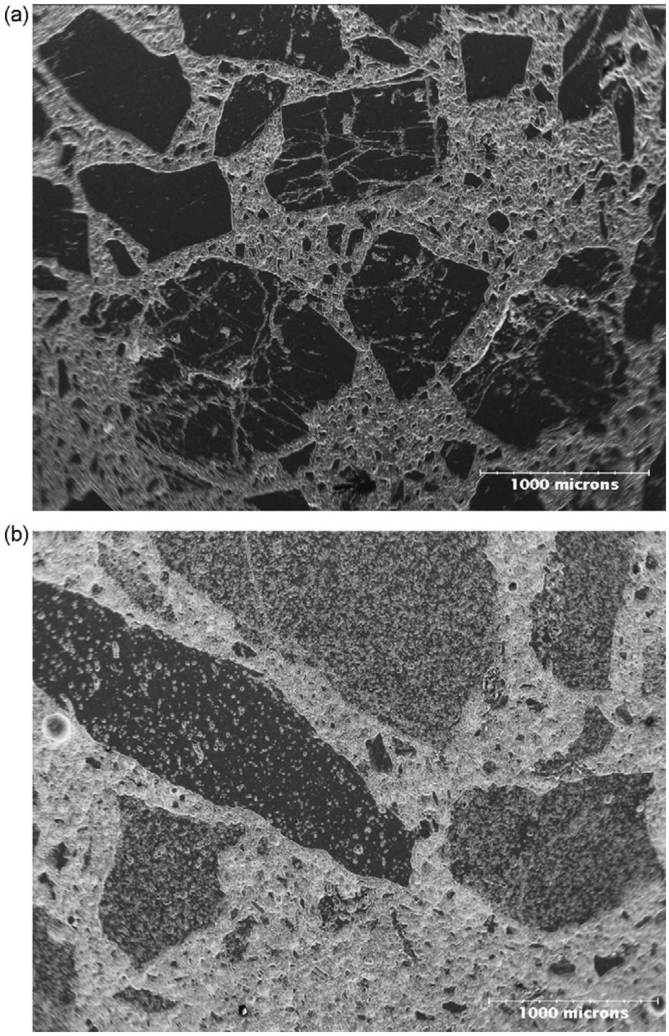

Fig. 1. Microstructure of studied refractories: (a) And-LCC; (b) Bau-ULCC.

### 2.3. Ultrasonic measurements

An ultrasonic technique based on a continuous in situ measurement of the velocity of longitudinal long bar mode waves in the material has been used to monitor the evolution of the elastic modulus versus temperature on both materials [13,14]. Fig. 2 is a schematic representation of the ultrasonic device. The determination of the ultrasonic velocity is based on the measurement of the round trip time $\tau$ between two successive echoes in the sample. The ultrasonic pulse is transmitted from the transducer to the sample through a waveguide. The measurement of the time $\tau$ between two successive echoes within the sample allows to calculate the wave velocity and then to obtain the value of the Young's modulus by $E_{us} = \rho(2L/\tau)^2$, where $L$ and $\rho$ are sample length and density, respectively.

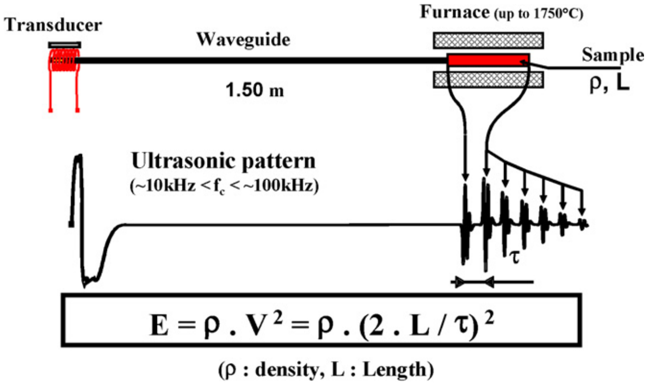

Fig. 2. Experimental set-up used for Young's modulus measurement at high temperature by long bar mode ultrasonic pulse technique.

### 2.4. Tensile test

Tensile tests have been performed with an INSTRON 8862 electro-mechanical universal testing machine at room temperature. Fig. 3 presents a schematic of the tensile test device. The strain is measured by two extensometers equipped by silicon carbide rods which are placed on two opposite faces of the specimen. The extensometer gauge length is 25 mm.

The low values of the displacement at rupture exhibited by these materials (3–5 μm) required a good control of the thermal stability of the extensometers (±0.1 °C). The refractory samples are constituted of a cylindrical rod (18 mm in diameter) glued to two metallic parts. The geometry is precisely adjusted thanks to a final cylindrical machining step of the total assembly. The tensile tests are carried out until rupture with a constant displacement velocity of 0.04 mm/min with intermediate unloading at several level of stress. To accurately determine the Young's modulus from tensile test results ($E_T$), the early slope of the first loading step of the stress–strain curves has been evaluated. Fig. 4 illustrates an example of stress–strain curve obtained on And-LCC treated at 110 °C and the method to determine the Young's modulus at the very first time.

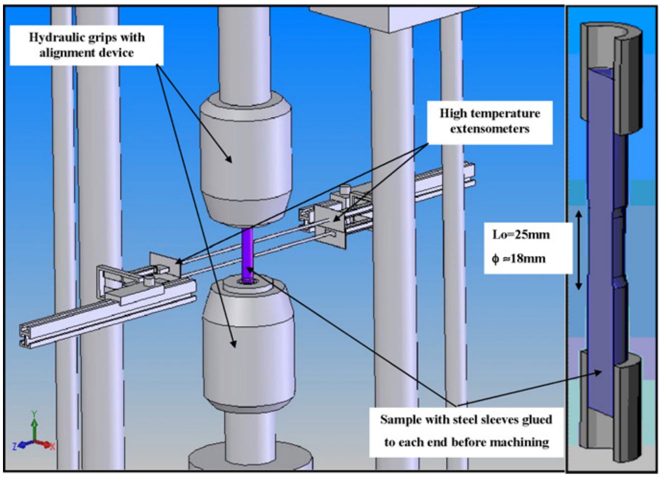

Fig. 3. Scheme of the tensile test device.

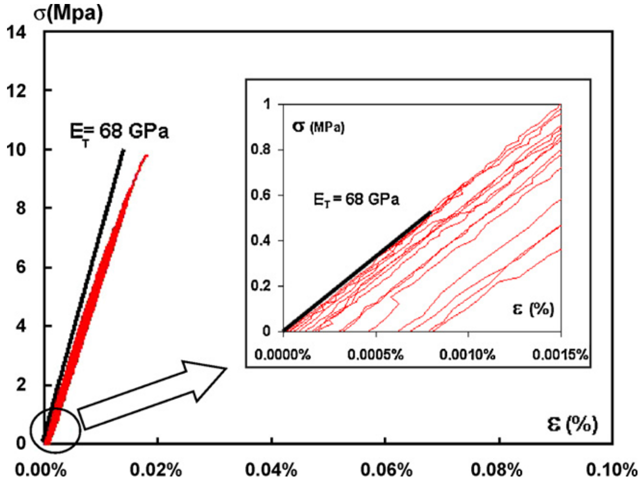

Fig. 4. Stress–strain tensile curves of And-LCC at room temperature after treatment at 110 °C. Zoom of the initial part of the curves that illustrates the early determination of the Young's modulus $E_T$.

## 3. Results and discussion

### 3.1. Young's modulus values at room temperature

For each method, except for the ultrasonic one, at least five samples were tested. Table 2 presents the results of the Young's modulus measured at room temperature by the two techniques (ultrasonic measurement and tensile test) on both castables. The obtained values are in good agreement within the experimental error.

In each case, a scatter of about 6% is observed from one sample to another. In addition, the bauxite-based castable, despite its higher porosity, is much stiffer than the andalusite one because of the higher intrinsic elastic properties of its aggregates.

### 3.2. Microstructural evolution during a first thermal cycle up to 1500 °C

Due to their compositions (natural aggregates and hydrated cementitous phases), different microstructural evolutions can take place during a first heating at high temperature. Young's modulus evolution coupled with dilatometric measurements was carried out (Fig. 5) in order to investigate these changes.

During the heating stage, between 150 °C and 350 °C, a strong decrease of $E$ occurs due to the dehydration of calcium aluminate hydrates from cement. In this temperature range, a slight decrease in thermal expansion is also observed. After this stage, $E$ slowly decreases as in a stable material up to 900 °C. Nevertheless, a slight inflection can be observed on the evolution of the Young's modulus for And-LCC around 600 °C, most probably related to the presence of quartz as impurity in andalusite aggregates (Fig. 5a), which undergo an $\alpha \rightarrow \beta$ crystallographic transition at 573 °C. The increase of the elastic modulus between 900 °C and approximately 1200 °C can be explained by the crystallisation of calcium aluminate and silicate phases (CA, $CA_2$ and $CAS_2$) [15] and, in addition, by mechanisms of sintering which can take place in this temperature range.

Table 2
Young's modulus at room temperature for the two castables

| Measurement method | And-LCC | | Bau-ULCC | |
|---|---|---|---|---|
| | Ultrasonic ($E_{us}$) | Tensile ($E_T$) | Ultrasonic ($E_{us}$) | Tensile ($E_T$) |
| Young's modulus at room temperature (GPa) | 62–70 | 65–75 | 95–100 | 91–100 |

The important reduction of the Young's modulus observed above 1200 °C for the two materials illustrates the beginning of their viscous behaviour, closely related to the occurrence of vitreous phases in this temperature range. For Bau-ULCC and in the same temperature domain, a slight shrinkage is marked on the dilatometric curve (Fig. 5b). This evolution is most probably related to the beginning of sintering of the smallest particles in the matrix. For And-LCC, the mullite formation, resulting in a strong expansion above 1350 °C (Fig. 5a), can superimpose this shrinkage on the dilatometric curve, due to its magnitude. These vitreous phases are also responsible of a strong attenuation of the waves, making difficult the ultrasonic measurements above 1300 °C.

During the cooling period, for both materials, Young's modulus firstly increases because of crack healing and sintering processes which have occurred at high temperature. Below 1000 °C, the materials behave like a stiff elastic ceramic, with a regular increase of the Young's modulus versus decreasing temperature. But at a given temperature ($T_C$; different for the two castables), the two materials exhibit a sudden decrease of $E$ because of damage due to thermal expansion mismatches between the different phases within the materials. However, this phenomenon is much less marked in the case of Bau-ULCC (Fig. 5b). In the And-LCC case, the Young's modulus at the end of the thermal cycle is always lower than that of the one measured at the beginning where the material is in its hydrated state.

### 3.3. *Young's modulus evolution during thermal cycles at lower temperatures*

Fig. 6 shows the evolution of the Young's modulus versus temperature for both castables during three thermal cycles carried out at different temperatures: 700 °C, 900 °C and 1100 °C. In the case of And-LCC, an evolution of the mechanical behaviour can be marked. In fact, and similarly to the cycle

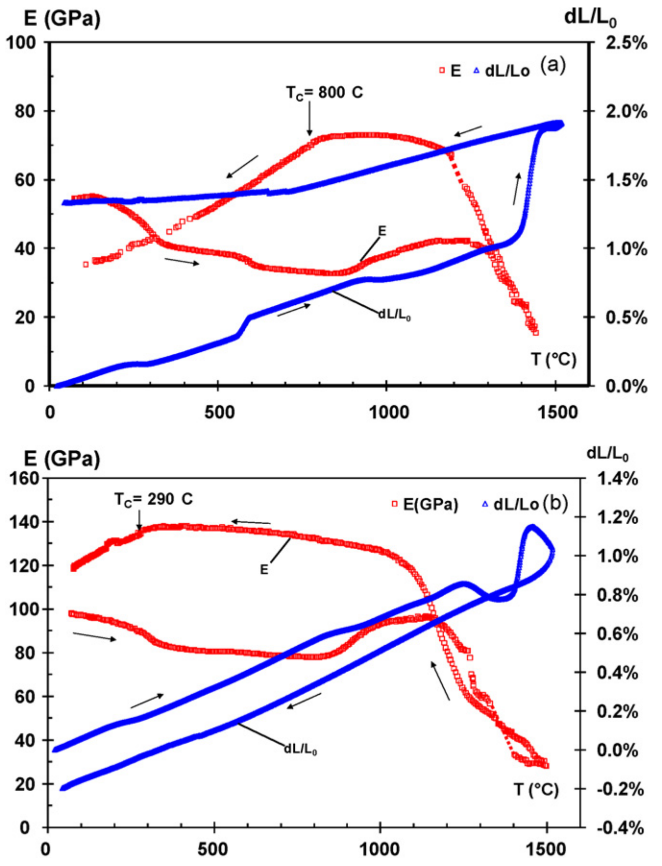

Fig. 5. Variation of the Young's modulus measured by the ultrasonic technique ($E_{us}$) and thermal expansion for the two castables: (a) And-LCC; (b) Bau-ULCC.

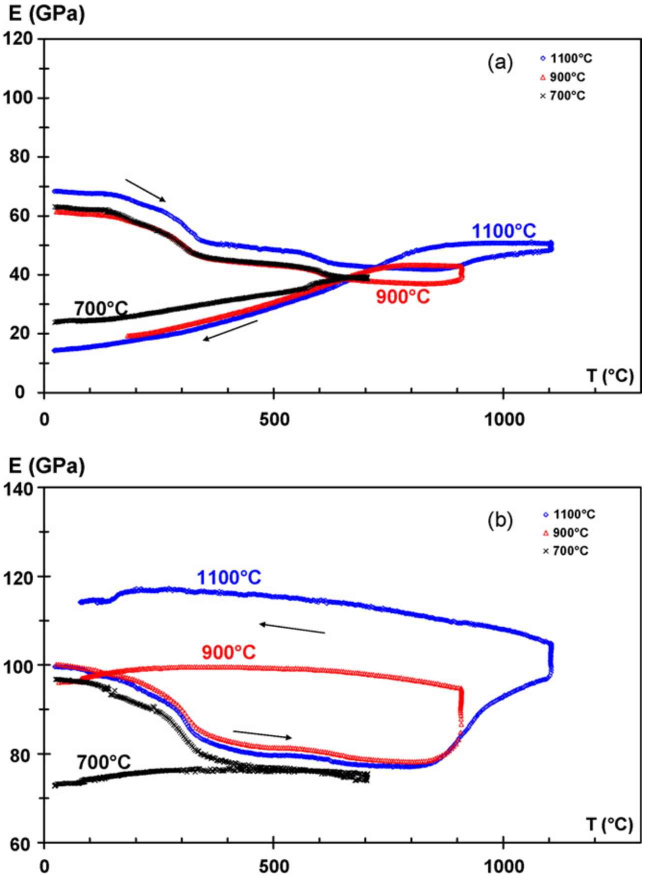

Fig. 6. Evolution of the Young's modulus measured by the ultrasonic technique ($E_{us}$) for both castables during different first thermal cycles: (a) And-LCC; (b) Bau-ULCC.

carried at 1500 °C, the final value of the Young's modulus after thermal cycles is always lower than that one taken at the beginning. But, a slight different interpretation can be given for the cycle carried out at 700 °C. For this thermal treatment, the material can be assumed as only dehydrated. It means that at 700 °C, the healing of microcracking or other sintering processes have not occurred yet. That is why after the dwell, one can observe the regular decrease of $E$ most probably due to the damage associated to the dehydration process (porosity growth, microcracking due to shrinkage, etc.). For higher temperatures and especially for 1100 °C, it seems that a partial recovering (especially during the temperature dwell) of the elastic properties has occurred. Indeed, at this temperature, it is most probable that a part of the recovering mechanisms previously quoted (healing, sintering) has taken place. This hypothesis is confirmed by the occurrence, during cooling, of a critical temperature ($T_C$) below which a significant drop of $E$ is observed. This decrease is closely related to the damage due to thermal expansion mismatches existing between phases within the material. This damage has been identified as decoherance between aggregates and matrix, and microcracks in the matrix (Fig. 7c).

In the case of the Bau-ULCC, the behaviour of the castable at 1100 °C approaches the one observed at 1500 °C, excepted the decrease of $E$ at high temperature due to the viscous behaviour. Healing of cracks at high temperature involves a large increase of Young's modulus during the soaking time. The behaviour of this material during the thermal cycle at 700 °C is similar to the one of And-LCC. In all cases, the Bau-ULCC castable is less damaged after cooling than the And-LCC one. The damage which occurs towards 300–250 °C during cooling is smaller and has been mainly identified as microcracks in the matrix (Fig. 7b and d).

### 3.4. Mechanical behaviour in tension after thermal treatment

Previous measurements have highlighted that elastic properties of the materials at room temperature could be strongly affected by the thermal history. The interest of the tensile tests is to supplement these data by the determination of mechanical behaviour laws, including the non-linear character of the material. Thus, tensile tests at room temperature were carried out on samples which had been previously treated at various temperatures (110 °C, 250 °C, 500 °C, 700 °C, 900 °C and 1100 °C) in order to investigate the influence of the thermal history on the mechanical behaviour of the two castables. These results are presented in Fig. 8. At the beginning of loading, the two materials present a linear elastic behaviour. Young's modulus ($E_T$) can be determined from the initial slope, measured between 0 MPa and 0.6 MPa, Table 3 compares the results of Young's modulus measured by the two different techniques.

Again, these results exhibit a good correlation between dynamic and static methods for the determination of the Young's modulus.

Beyond the linear elastic domain, the two materials exhibit a non-linear behaviour. In one hand, it is very limited in the case of Bau-ULCC, and, in the other hand, it is much extended in

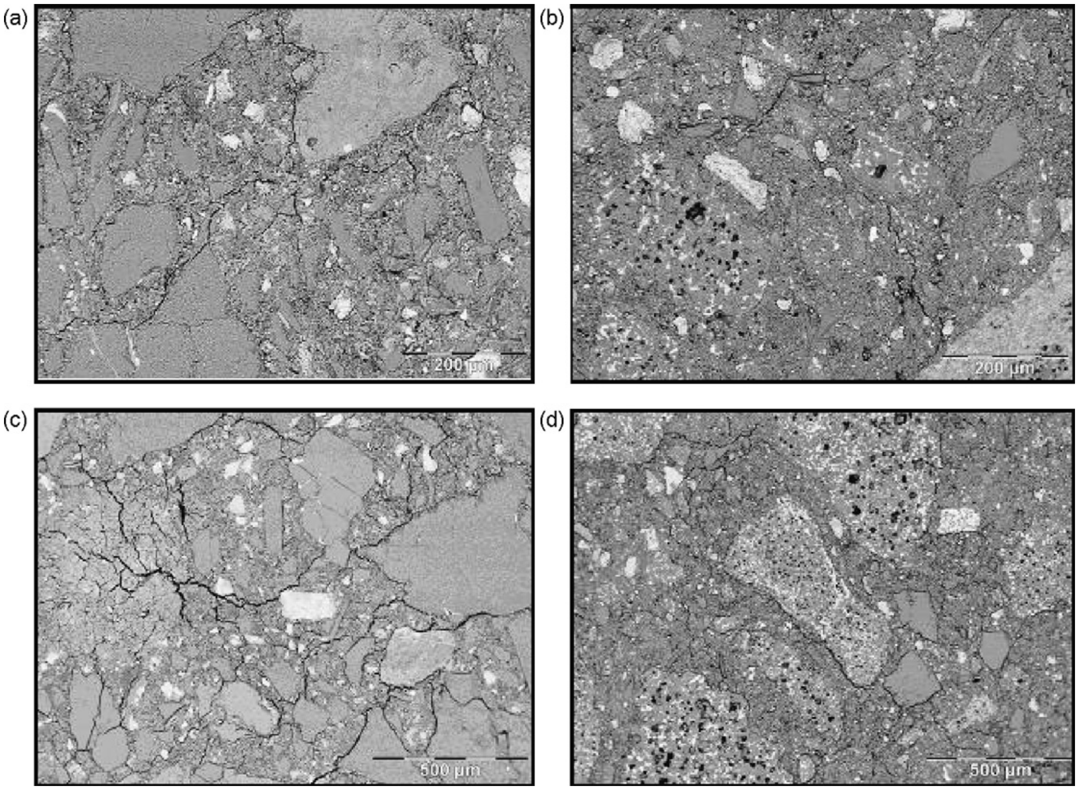

Fig. 7. Identification of damage in the two castables after thermal treatments: (a) And-LCC at 700 °C; (b) Bau-ULCC at 700 °C; (c) And-LCC at 900 °C; (d) Bau-ULCC at 900 °C.

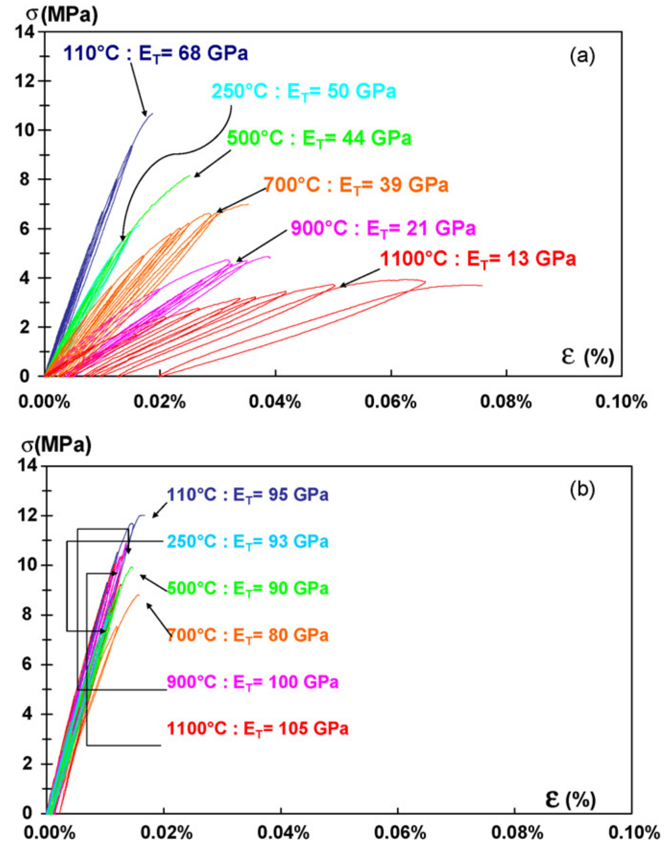

Fig. 8. Tensile behaviour at room temperature of both castables treated at different temperatures: (a) And-LCC; (b) Bau-ULCC.

the case of And-LCC. After these observations, tensile results emphasise:

- the high rigidity of the bauxite-based castable;
- the reduction of the Young's modulus ($E_T$) after thermal treatments in the case of the And-LCC castable;
- The increase of the Young's modulus (above 700 °C) after thermal treatments in the case of Bau-ULCC.

After the treatment at 110 °C, the And-LCC castable exhibits a rather linear elastic behaviour. Then, as the temperature of treatment shifts to higher values, the behaviour moves from a linear elastic one to a non-linear one (Fig. 8a). The magnification of his non-linear behaviour is most probably due to microcracking mechanisms which have been previously occurred during the cooling stage of the associated thermal treatment. As temperature increases, $E_T$ decreases (from 68 GPa after a treatment at 110 °C to 13 GPa after a treatment at 1100 °C). In the same time, the strain-to-rupture increases notably (from 0.018% to 0.074%).

Table 3
Comparison of the Young's moduli obtained at room temperature by two different techniques (ultrasonic and tensile test) for both castables previously treated at different temperatures

| Temperature of treatment (°C) | And-LCC | | Bau-ULCC | |
|---|---|---|---|---|
| | $E_{us}$ (GPa) | $E_T$ (GPa) | $E_{us}$ (GPa) | $E_T$ (GPa) |
| 110 | 62–70 | 65–75 | 95–100 | 91–100 |
| 250 | – | 49–53 | – | 91–96 |
| 500 | – | 46–50 | – | 86–91 |
| 700 | 21–25 | 36–43 | 73–75 | 75–89 |
| 900 | 14–17 | 18–24 | 94–96 | 95–104 |
| 1100 | 10–15 | 8–15 | 110–115 | 96–121 |

In the case of Bau-ULCC castable, the amplitude of evolution of $E_T$ is much more limited (Fig. 8b). Moreover, it seems that a reversion of tendency, concerning this parameter, appears for thermal treatments carried out above 700 °C. In fact, as temperature increases (up to 700 °C), $E_T$ decreases regularly (from 95 GPa after a treatment at 110 °C to 80 GPa after a treatment at 700 °C). In the same time, strain-to-rupture slightly increases (from 0.012% to 0.016%). On the contrary, above 700 °C, $E_T$ increases (from 80 GPa after a treatment at 700 °C to 105 GPa after a treatment at 1100 °C). This increase of Young's modulus above this temperature can be explained as follow: The presence of some impurities inside bauxite aggregates ($TiO_2$, $Fe_2O_3$ and $K_2O$), induces the formation of vitreous phases promoting sintering processes at high temperature and stiffening the material (Fig. 6b).

### *3.5. Source of damage in the castables*

As previously presented, the studied castables are constituted of matrix and aggregates. In this kind of heterogeneous materials, the significant reduction of their Young's modulus during cooling associated to a non-linear behaviour in tension after thermal treatment often find their origin in the existence of damage mechanisms induced by thermal expansion mismatch between the constitutive phases [16]. In order to understand these mechanisms on both castables better, a study has been carried out on the dilatometric properties of the aggregates and of the matrix, separately considered. Samples of matrix were prepared by casting. For bauxite aggregates, because thermal expansion experimentation could not be performed on simple aggregates and due to the polycrystalline character of these last, compact of aggregates have been prepared by uniaxial pressing. For andalusite aggregates, as they are mainly single crystals, the study has been carried out on single crystals thanks to chiastolite obtained from an Iranian deposit (ASACO Company, Iran) which offers the advantage to be available in a much larger grain size with similar chemical composition than those present in the castable (Kerphalite from DAMREC, Glomel, France).

The results obtained for Bau-ULCC (Fig. 9) show the thermal expansion behaviour of the two components of this castable. The thermal expansion coefficients, measured between 900 °C and 450 °C after sintering at 1200 °C are $9.0 \times 10^{-6}\,K^{-1}$ for the bauxite aggregates and $7.6 \times 10^{-6}\,K^{-1}$ for the matrix. This slight difference could explain the damage observed by ultrasonic measurement during the cooling stage at $T < T_C$.

In the case of And-LCC castable, it has been reported that the orthorhombic structure of the andalusite single crystal can induce a thermal expansion anisotropy [17] of this last. Thus, a specific study has been carried out on large size andalusite aggregates where different samples have been extracted (Fig. 10)

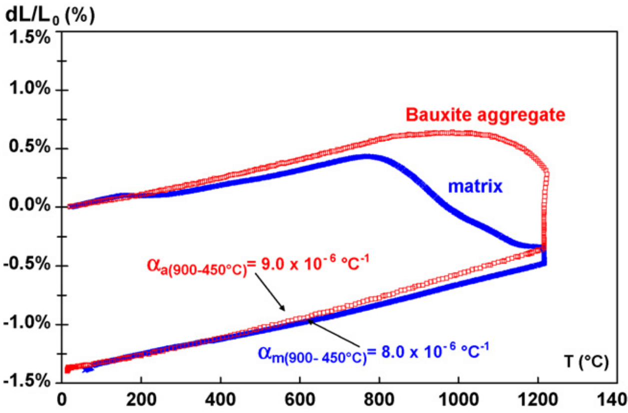

Fig. 9. Thermal expansion behaviours obtained on the bauxite aggregates and the matrix of Bau-ULCC castable.

Table 4
Thermal expansion coefficients of andalusite aggregates and matrix of the And-LCC castable between 900 °C and 450 °C ($\times 10^{-6}$ °C$^{-1}$)

| Matrix | Andalusite aggregates (single crystal) | | |
|---|---|---|---|
| | $\vec{a}$ | $\vec{b}$ | $\vec{c}$ |
| 7.6 | 12.9 | 9.6 | 3.1 |

in order to investigate the thermal expansion along the principal directions of these aggregates. The values of the thermal expansion coefficients (Table 4), measured between 900 °C and 450 °C, for both andalusite aggregates, according to the three axis of the single crystal, and for the matrix, are presented in Fig. 11. In this figure, one can easily observe the large thermal expansion mismatch existing, for example, between the matrix ($\alpha_{\mathrm{m}} = 7.6 \times 10^{-6}\,\mathrm{K}^{-1}$) and the andalusite aggregate taken as well along the $\vec{a}$ axis ($\alpha_{\vec{a}} = 12.9 \times 10^{-6}\mathrm{K}^{-1}$) as along the $\vec{c}$ axis ($\alpha_{\vec{c}} = 3.1 \times 10^{-6}\mathrm{K}^{-1}$). These results highlight the very large difference that can be observed between the thermal expansion behaviour of two different constituents mixed in the same castable and allow to explain the origin of the strong damage observed during the cooling stage (at $T < T_{\mathrm{C}}$) in the andalusite-based castable.

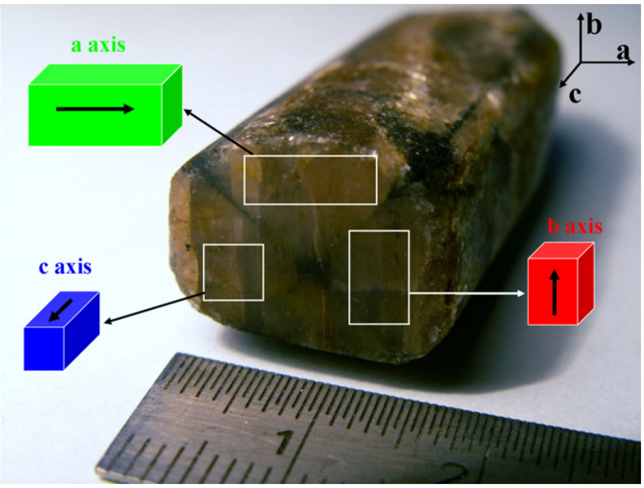

Fig. 10. Scheme of the dilatometric sample extraction procedure applied on an andalusite single crystal to investigate its thermal expansion anisotropy.

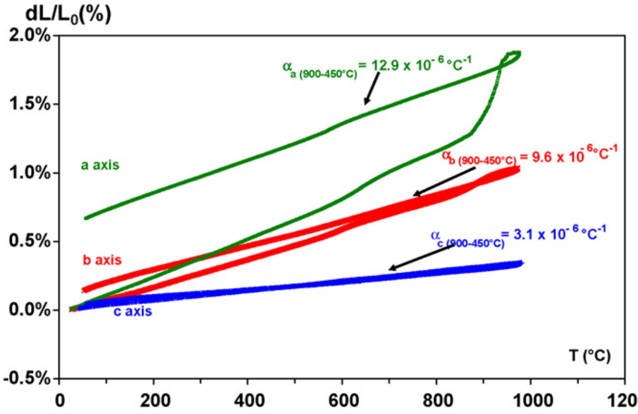

Fig. 11. Comparison of the dilatometric behaviour in the three directions of an andalusite single crystal with the matrix of the And-LCC castable.

## 4. Conclusion

Both castables exhibit notable damage behaviours with a damage level related to the firing temperature. The tensile behaviour is characterised by a linear elastic domain at the beginning of loading followed by a non-linear evolution up to the peak. For a same temperature, the extend of the non-linear domain for the And-LCC castable is higher than for the Bau-ULCC one because of damage development. In the case of the andalusite castable, temperature cycling reduces the maximum strength, but strongly increases the compliance and the strain-to-rupture, thanks to microstructure effects related to andalusite aggregates (damage onset and propagation due to thermal expansion mismatch between aggregates and matrix related to the anisotropic dilation of andalusite). One could take advantage of these last two mechanical properties for the enhancement of thermal shock resistance of such refractory castables.

## Acknowledgements

One part of this work was carried out in the framework of the French National Research Program PROMOTHEREF on refractory materials. The authors are grateful to the French Ministry of Economy and Industry for its financial support. Authors would like to thank TRB Refractories Company for supplying the studied castables and Iranian ASACO Company for supplying the andalusite single crystals. One author, Dr. Ghassemi-Kakroudi, is particularly thankful to the Iranian Ministry of Science and Technology and to the University of Tabriz for financial support.

## References

[1]. Lee, W. E., Evolution of in situ refractories in the 20th century. *J. Am. Ceram. Soc.*, 1998, **81**(6), 1385–1410.
[2]. Ningsheng, Z., Advances in modern refractory castables. In *Proceedings of the First International Conference on Refractories*, 2004, pp. 148–154.
[3]. Serry, M. A. and Telle, R., Thermomechanical properties of high alumina castables. *Am. Ceram. Bull.*, 2000, **79**(11), 71–75.

[4]. Auvray, J. M., Gault, C. and Huger, M., Evolution of elastic properties and microstructural changes versus temperature in bonding phases of alumina and alumina–magnesia refractory castables. *J. Eur. Ceram. Soc.*, 2007, **27**, 3489–3496.

[5]. Givan, G. V., Hart, L. D., Heilich, R. P. and MacZura, G., Curing and firing of high-purity calcium aluminate-bonded tabular alumina castables. *Am. Ceram. Bull.*, 1975, **54**(8), 710–713.

[6]. Criado, E., Estrada, D. A. and DeAza, S., Dilatometric study of the formation of CA2 and CA6 in cements and refractory concretes. *Special Bull. Ceram. Glass. Soc.*, 1976, **15**(5), 319–321.

[7]. Chotard, T., Smith, A., Rotureau, D., Fargeot, D. and Gault, C., Acoustic emission characterisation of calcium aluminate cement hydration at an early stage. *J. Eur. Ceram. Soc.*, 2003, **23**, 387–398.

[8]. Parr, C., The impact of calcium aluminate cement hydration upon the properties of refractory castables. *J. Tech. Assoc. Refract.*, 2005, **25**(2), 78–88.

[9]. Midgley, H. G., In *Calcium Aluminate Cements*, ed. R. J. Mangabhai. Chapman and Hall, London, 1990, pp. 1–13.

[10]. Tessier-Doyen, N., Glandus, J. C. and Huger, M., Untypical Young's modulus evolution of model refractories at high temperature. *J. Eur. Ceram. Soc.*, 2006, **26**, 289–295.

[11]. Meschke, G., Lackner, R. and Mangan, H. A., Anisotropic elastoplastic-damage model for plain concrete. *Int. J. Numer. Methods Eng.*, 1998, **42**, 703–727.

[12]. Gajda, J. and McGee, T. D., Elastic properties of a calcium aluminate cement based concrete. *Am. Ceram. Bull.*, 1997, **76**(4), 81–85.

[13]. Gault C, Ultrasonic non destructive evaluation of microstructural changes and degradation of ceramics at high temperature. In *Proceedings of the American Material Research Symposium*, ed. J. Holbrook and J. Bussiere, 1989, pp. 263–274.

[14]. Huger, M., Fargeot, D. and Gault, C., High-temperature measurement of ultrasonic wave velocity in refractory materials. *High Temp.-High Press.*, 2002, **34**, 193–201.

[15]. Marzagui, H. and Cutard, T., Characterization of microstructural evolutions in refractory castables by in situ high temperature ESEM. *J. Mater. Proc. Tech.*, 2004, **156**(11), 1474–1481.

[16]. Huger, M., Tessier-Doyen, N., Chotard, T. and Gault, C., Microstructural effects associated to CTE mismatch for enhancing the thermal shock resistance of refractories: investigation by high temperature ultrasounds. *Ceram. Forum. Int.*, 2007, **9**, E93–E102.

[17]. Winter, J. K. and Ghose, S., Thermal expansion and high-temperature crystal chemistry of the $Al_2SiO_5$ polymorphs. *J. Am. Mineral.*, 1979, **64**, 573–586.